

1 **Polyploidy and plant-fungus symbiosis: evidence of cytotype-specific microbiomes in the halophyte**

2 ***Salicornia* (Amaranthaceae)**

3

4 Danilo Reis Gonçalves¹, Rodica Pena² & Dirk C. Albach¹

5 ¹Institute for Biology and Environmental Sciences, Carl von Ossietzky University of Oldenburg, Germany

6 ²Department of Sustainable Land Management, University of Reading, United Kingdom

7

8 **Corresponding author:** danilo.reis.goncalves1@uni-oldenburg.de

9

10 **Abstract**

11 Polyploidy is recognized as a mechanism of speciation in plants with cascading effects on biotic interactions.

12 However, a limited number of studies have investigated the effects of polyploidy on the association of plants

13 and microorganisms. Herein, we investigated whether two *Salicornia* cytotypes (*S. europaea* – 2x and *S.*

14 *procumbens* – 4x) show different root-associated fungal communities. Additionally, we explored the existence of

15 cytotype-specific root anatomical traits, which could influence fungal recruitment and establishment. *Salicornia*

16 spp. were identified based on their ploidy level. The root-associated fungal microbiome of *Salicornia* was

17 analyzed using high throughput amplicon sequencing (ITS1 of rDNA) in spring and summer. The following root

18 anatomical traits were investigated: maximum root diameter, periderma thickness, parenchyma thickness,

19 diameter of the vascular cylinder and maximum diameter of parenchyma cells. Our results showed that Shannon

20 diversity and evenness indices were higher in samples of *Salicornia procumbens* (4x) compared to those of *S.*

21 *europaea* (2x), and in summer the root-associated fungal community of *S. procumbens* (4x) was significantly

22 different from that of *S. europaea* (2x). The orders *Xylariales*, *Malasseziales* and *Pleosporales* were the most

23 frequent root colonizers in both cytotypes and most of the taxa associated with *Salicornia* were functionally

24 classified as saprophytes or plant pathogens. Finally, we observed larger periderma and parenchyma layers in *S.*

25 *procumbens* (4x) than *S. europaea* (2x) that may contribute to the observed differences in community

26 composition between the two cytotypes. Our results suggest that differences in ploidy may modulate plant

27 interaction with fungi by affecting species recruitment and microbiome structure. In addition, cytotype-specific

28 root traits may also have the potential to affect differently community assembly in the two cytotypes.

29

30 **Keywords:** plant-microbe interactions, endophytic fungi, mycobiome, polyploidy, salt marsh plants

31 **Introduction**

32 Among the different factors controlling species interactions, polyploidy or whole-genome duplication is
33 considered an important yet underexplored process (Segraves & Anneberg 2016). The genetic changes caused
34 by polyploidization in plants may have effects on cell biology (Doyle & Coate 2019), plant chemistry
35 (Corneillie et al. 2019; Veach et al. 2018), physiology (Baker et al. 2017) and anatomy (Chansler et al. 2016).
36 These changes have been shown to produce cascading effects on biotic interactions, for example, on plant-
37 pollinator (Husband and Schemske 2000; Kennedy et al. 2006) and plant-herbivore associations (Collins &
38 Müller-Schäfer 2012; Kao 2008). As an example, Edger et al. (2015) reported that the presence of
39 glucosinolate defensive compounds in polyploid individuals of Brassicales might negatively impact herbivory.
40 In the same way, an increase in the production of defense compounds in polyploids may negatively affect
41 colonization by endophytic fungi (Segraves & Anneberg 2016; van Loon et al. 2006). However, associations of
42 plants and microorganisms have been investigated in only a very limited number of studies, with controversial
43 outcomes despite the prominent effect of microorganisms on the growth and survival of plants.

44

45 Investigations of potential effects of polyploidy on plant-microbe interactions are limited to bacteria (Cavé-
46 Radet et al. 2020; Forrester & Ashman 2018, Forrester & Ashman 2019; Wipf & Coleman-Derr 2021) and
47 arbuscular mycorrhizal fungi (AMF) (Annenberg & Seagraves 2019; Sudová et al. 2010; Sudová et al. 2014;
48 Sudová et al. 2018; Těšitelová et al. 2013). For instance, microscopical analyses have shown that AMF
49 colonization in tetraploid individuals of *Heuchera cylindrica* was higher compared to diploids (Anneberg &
50 Segraves 2019) and more diverse AMF communities were observed in tetraploid individuals of *Gymnadenia*
51 *conopsea* compared to diploids (Těšitelová et al. 2013). In contrast, two other studies showed no correlation of
52 ploidy and AMF colonization in *Aster amellus* (Sudová et al. 2014) and *Centaurea stoebe* (Sudová et al. 2018).
53 Importantly, none of these studies investigated the dynamics of colonization throughout different seasons. Thus,
54 any general conclusions on the effects of polyploidy in shaping plant-fungus association in a broader context are
55 currently not possible.

56

57 Despite the reported differences in microorganism colonization between diploid and polyploid plants, the
58 underlying differences in anatomical, physiological or chemical processes directly affecting the plant-AMF
59 interaction have not been explored in previous studies and are largely unknown. In the case of bacteria, this has
60 started to be elucidated. Micallef et al. (2019) observed that in *Arabidopsis thaliana*, the different exudation

61 patterns observed in different cytotypes directly influenced bacterial recruitment and community assembly,
62 which could also be occurring with fungi. In addition, root anatomical traits likely play a role by affecting
63 bacterial and fungal microbiome assembly. For example, Galindo-Castañeda et al. (2019) reported less
64 mycorrhizal colonization in roots of individuals of *Zea mays* with a smaller living cortical area.

65

66 An interesting model organism to study the effects of polyploidy on species interactions is the halophyte
67 *Salicornia*. In this genus, fungal symbionts, especially of the order *Pleosporales* (Ascomycota), are reported in
68 the roots (Furtado et al. 2019a) and were shown to positively affect nutrient uptake and plant growth (Gonçalves
69 et al. 2021). In northern Germany, two different but closely related *Salicornia* cytotypes occur, *Salicornia*
70 *europaea* (2x) and *Salicornia procumbens* (4x). The two species have a similar morphology and react highly
71 plastic to changes in the environment, which makes morphology-based species identification challenging and
72 time-consuming. In addition to that, there are no studies investigating whether the two cytotypes differ in root
73 anatomical traits, which could directly influence fungal recruitment and community establishment, as observed
74 for endophytic bacteria (Forrester et al. 2020) and fungi (Galindo-Castañeda et al. 2019). Because of the
75 morphological similarities of the cytotypes, species identification is mostly conducted based on their differences
76 in ploidy (Kadereit et al. 2007). Although the broadest phylogenetic study of the genus *Salicornia* (Kadereit et
77 al. 2007) suggested that both cytotypes are phylogenetically not sister, a recent study by Buhk (2020) using
78 genotyping-by-sequencing across the western part of the German Wadden Sea, revealed a high genetic similarity
79 and sharing of alleles between the cytotypes. Thus, the data by Buhk (2020) suggest an autopolyploid origin of
80 *S. procumbens* by autopolyploidy from *S. europaea* or a genetically similar species.

81

82 Both cytotypes occur sympatrically but are differentiated on a microscale in the salt marsh zones. *Salicornia*
83 *europaea* (2x) is mostly present in the lower salt marsh but also reported in the pioneer zone. On the other hand,
84 *S. procumbens* (4x) seem to be more evenly distributed in the salt marsh zones and tidal flat, except in the upper
85 salt marsh where both cytotypes do not occur. Interestingly, an ecologically differentiated distribution of two
86 *Salicornia* species (*S. procumbens* and *S. stricta*) in the salt marsh zones was observed by Teege et al. (2011)
87 with *S. procumbens* growing in the lowest parts of the salt marsh. The authors suggested a strong selection
88 during seed germination and establishment as a reason for the existence of intraspecific ecotypes. Nevertheless,
89 there is no information available on the role of belowground interactions regarding habitat differentiation

90 between diploids and tetraploids, although it has been shown to influence habitat differentiation of plant species
91 (Reynolds et al. 2003).

92

93 There are studies showing that in order to synthesize additional chromosomal sets, polyploids have a higher
94 demand for nitrogen and phosphorus compared to diploids (Šmarda et al. 2013; Wildermuth 2010). This may
95 have consequences for the association of plants with beneficial fungi. For example, Anneberg & Segraves
96 (2019) observed a higher number of nutritional-exchange structures of AMF in roots of the tetraploid *Heuchera*
97 *cylindrica* compared to diploids. In the case of *Salicornia*, in which AMF have been reported to be absent in the
98 roots (Furtado et al. 2019a), polyploidy may have further consequences in plant's interaction with another group
99 of endophytic fungi, dark septate endophytes (DSE). Fungi classified as DSE are mainly found in the orders
100 Pleosporales, Xylariales and Helotiales of the Ascomycota (Knapp et al. 2018), are commonly found in roots of
101 salt marsh plants (Furtado et al. 2019a; Maciá-Vicente et al. 2016) and are known for their ability to improve
102 plant growth (Mateu et al. 2020; Vergara et al. 2019). In this sense, it is possible that *S. procumbens* (4x)
103 benefits from the association with a more diverse fungal community, especially of mutualistic DSE, to survive
104 in the lowest parts of the salt marsh. In addition, the fitness benefits conferred by DSE in halophytes, such as
105 salt stress tolerance (Mateu et al. 2020), may contribute to the adaptation of *S. procumbens* (4x) to more stressed
106 areas (e.g., tidal flats), where frequent flooding associated with high salinity occur. Plant phenology is a major
107 driver of plant ability to acquire soil resources (Nord & Lynch, 2009). Therefore, the fungal contribution in plant
108 nutrient acquisition may vary with the season. Surprisingly, Furtado et al. (2019a) and Maciá-Vicente et al.
109 (2016) did not observe seasonal changes in fungal communities colonizing *Salicornia europaea* and *S. patula*.
110 However, we considered this surprising and aimed to confirm whether differences in host ploidy are potentially
111 playing a role in seasonal variation.

112

113 Using a high-throughput amplicon sequencing technique, we investigated whether cytotype-specific fungal
114 microbiomes occur in *Salicornia*. For this purpose, individuals of *S. europaea* (2x) and *S. procumbens* (4x)
115 occurring in mixed-ploidy populations in the lower zone of a salt marsh located on the island of Spiekeroog
116 (Germany) were collected during the spring and summer of 2020. We hypothesized that (i) *S. procumbens* (4x)
117 has a more diverse root-associated endophytic fungal microbiome compared to *S. europaea* (2x), (ii) mutualistic
118 fungi are more abundant in roots of *S. procumbens* (4x) than *S. europaea* (2x), and finally (iii) the observed
119 patterns in microbiome composition are stable over two different sampling seasons. Additionally, we

120 investigated whether *S. europaea* (2x) and *S. procumbens* (4x) show differences in root anatomical traits (e.g.,
121 cell size) which could impact differently fungal recruitment and microbiome assembly in the two cytotypes.

122

123 **Material and Methods**

124 **Study area and sampling**

125 Sampling was performed during spring (early June) and summer (late August) of 2020 in the lower zone of a
126 salt marsh located within the limits of the Wadden Sea National Park on the island of Spiekeroog, Germany
127 (53°45'N 7°43'E). Sampling was performed in the lower salt marsh (LSM) where *Salicornia europaea* (2x) and
128 *S. procumbens* (4x) co-occur in mixed-ploidy populations. We focused our sampling on one population and one
129 salt marsh zone in order to reduce potential cofounding effects of a larger scale spatial heterogeneity, dispersal
130 limitation and local adaptations on the structure of the fungal microbiomes associated to each cytotype. To
131 characterize the study area, the elemental chemical composition of a composite soil sample of each season
132 (collected at three different points) was analysed (Table S1) at the Institute for Soil and Environment, Lufa
133 Nord-West (Oldenburg, Germany).

134

135 We know from previous analyses (Buhk 2020) that position within the salt marsh has a significant influence on
136 the root microbiome of both *Salicornia* species. We, therefore, sampled both cytotypes in close proximity and
137 overlapping root space. At the first sampling event (spring), 21 sampling points were randomly marked in the
138 LSM (at least five meters apart from each other) and five individuals occurring side by side were collected at
139 each point. Plants were carefully cleaned from the soil, large soil particles were removed from the root system
140 and afterwards, each individual was placed in a separate plastic bag, labelled and kept at 4°C until further
141 processing in the laboratory. In the summer, the sampling was performed identically, and individuals were
142 collected at the same sampling points established in spring. In total, 100 individuals of unknown ploidy were
143 collected in each season in order to maximize the chances of collecting a significant number of plants belonging
144 to each cytotype.

145

146 In the laboratory, the roots and shoots of each individual were separated and processed separately. Shoots were
147 washed, placed in plastic bags and kept at 4°C for a maximum of one week before genome size determination.
148 Roots were washed to remove any adhering soil particle, cut in small pieces of about 1 cm and posteriorly, root

149 pieces were surface sterilized following the protocol described in Crous et al. (2009). After that, the roots were
150 kept at -20°C until DNA extraction.

151

152 **Genome size estimation and ploidy determination**

153 For genome size estimation, the protocol described in Baranyi & Greilhuber (1996) was followed.
154 Approximately 1 cm of shoots of sampled individuals was chopped with the same amount of an internal
155 standard (*Hedychium gardnerianum*; 1C=2.01 pg; Meudt et al. 2015) into a homogenous mass by using a razor
156 blade in a petri dish, containing 550 µl nuclei extraction buffer (OTTO I). After that, another 550 µl of the
157 buffer was added to the sample suspension and filtered through a 30 µm CellTric filter (Partec GmbH, Münster,
158 Germany) into a plastic tube, followed by the addition of 50 µl 5% RNase. Samples were incubated in a water
159 bath for 30 min at 37 °C. After that, 450µl of the cell suspension was transferred to a new plastic tube
160 containing 2 mL of 6% propidium iodide staining solution. Staining was carried out in the darkness for one hour
161 at 4°C. Genome size was determined in a CyFlow SL flow cytometer (Partec GmbH, Münster, Germany)
162 equipped with a green laser (532 nm, 30 mW) as an excitation light source. Five thousand particles were studied
163 and only measurements with coefficients of variation (CVs) < 5% were considered. However, for some
164 individuals, measurements with CVs of 5–8% were also included. Ploidy measurements were performed until at
165 least 20 individuals of each ploidy in each season was obtained. The distribution of each cytotype according to
166 the different sampling points is shown in Table S2.

167

168 **Root anatomical investigation**

169 In order to investigate whether *S. europaea* (2x) and *S. procumbens* (4x) show differences in root anatomical
170 traits, additional samples of each cytotype were collected in the LSM and the ploidy level was estimated for
171 species identification (Table S3). Root samples were washed under tap water and stored individually in ethanol
172 (70%). For each cytotype, 10 individuals were selected and two root cuts of the primary root of each individual
173 were obtained and used to measure the following anatomical parameters: maximum root diameter, periderma
174 thickness, parenchyma thickness, diameter of the vascular cylinder and maximum diameter of parenchyma cells.
175 Microscope slides were prepared, and measurements were performed using the software Olympus CellSens
176 Entry 2.2 (Olympus Cooperation, Tokyo, Japan) under a Reichert-Jung Polyvar (Reichert, Wien, Austria)
177 transmitted light microscope. For statistical analysis, a one-way ANOVA was performed, followed by a Tukey

178 test to identify differences among cytotypes. Statistical analyses were performed in R (version 3.6.3, R
179 Development Core Team, 2011).

180

181 **DNA extraction, PCR, library preparation and sequencing**

182 DNA was extracted from 40 composite root samples (ten of each cytotype collected in each season). Roots of
183 two individuals of the same ploidy that occurred in the same sampling point were grouped to form a composite
184 sample for DNA extraction. In the case that only one diploid or tetraploid *Salicornia* was detected in a specific
185 sampling point, a composite sample was formed with two samples of the same ploidy collected in different
186 sampling points. This was performed due to the low root biomass content of some samples, especially those
187 collected in spring. Before DNA extraction, root samples (approximately 20 mg) were lyophilized in an Alpha
188 1-2 LDplus freeze-dryer (Martin Christ Gefriertrocknungsanlagen GmbH, Germany) for 24 hours. The
189 lyophilized samples were powdered using a Mixer Mill (Retsch, Germany) for two cycles of 1 min each with 30
190 oscillations per second. Genomic DNA was extracted using the innuPREP Plant DNA Kit (Analytic Jena AG,
191 Jena, Germany), following the manufacturer's instructions. The concentration and quality of extracted DNA
192 were checked by absorption spectrophotometry with a Tecan Infinity 200 PRO microplate reader (Tecan Group
193 Ltd., Männedorf, Switzerland). Dilutions for each sample were prepared to achieve a final concentration of 2 ng
194 μl^{-1} .

195

196 For the amplification of the ITS1 region of nrDNA, the primers ITS1FKyo2 (Toju et al. 2012) and ITS86R
197 (Vancov & Keen 2009), which target all major fungal groups, were used. Each sample was amplified in
198 duplicates and the reaction was prepared in a volume of 25 μl containing: 1.0 μl of DNA (2 ng μl^{-1}), 5 μl of 5x
199 Phusion Buffer, 0.6 μl of MgCl², 0.5 μl 10 mM dNTPs, 0.5 μl of each primer (10 pmol μl^{-1}), 0.2 μl of Phusion
200 Hot Start Flex DNA polymerase (New England Biolabs GmbH) and 16.7 μl of nuclease-free water. PCR
201 parameters were based on Maciá-Vicente et al. (2020) with minor adaptations: an initial step of 98°C for 1 min
202 and 3 cycles of 98°C for 30 s, 55°C for 30 s and 72°C for 30 s. The further 32 cycles consisted of 98°C for 30 s,
203 55°C for 30 s, and 72°C for 30 s. The elongation step was at 68°C for 10 min. After amplification, products of
204 the two reactions were pooled together and used in a second PCR reaction to ligate the adapters. This reaction
205 was performed accordingly: an initial step of 98°C for 1 min and 7 cycles of 98°C for 30 s, 55°C for 30 s and
206 72°C for 30 s followed by an elongation step at 68°C for 10 min. PCR products were checked on a 1.2% agarose

207 gel stained with ethidium bromide (Sigma-Aldrich). Subsequently, amplicons were sequenced at LGC
208 Genomics (Berlin, Germany) in an Illumina MiSeq platform (V3 chemistry, 300 bp paired-end reads).

209

210 **Bioinformatics and statistical analyses**

211 Sequence data was analysed and visualized using QIIME2 v.2020.11 (Bolyen et al. 2019). Demultiplexed
212 sequences were processed using ITSxpress plugin (Rivers et al. 2018), which implements ITSx and BBMerge
213 (Bushnell et al. 2017). Default parameters were used to run ITSxpress. Afterwards, reads were further processed
214 using DADA2 denoise.paired plugin to identify exact amplicon sequence variants (ASVs) rather than lumping
215 sequence variants to OTU's (Callahan et al. 2017). Taxonomic assignments were performed using qiime
216 feature-classifier classify-sklearn with a pre-trained Naïve-Bayes classifier using the database UNITE (version
217 v.8.2) (Abarenkov et al. 2020). Amplicon sequence variants that were assigned to plants and protists were
218 removed from the final ASV table. For functional assignment, a table containing the genera occurring in each
219 cytotype was used and compared with the information available in the FungalTraits (Põlme et al. 2021) and
220 FunGuild (Nguyen et al. 2016) databases.

221

222 In order to confirm whether sampling depth was sufficient, rarefaction curves were generated in QIIME2 using
223 the qiime.diversity.alpha-rarefaction plugin. Differences in sampling depth were accounted by rarefying samples
224 to a sampling depth of 1000 sequences before proceeding with diversity analyses. Alpha diversity was estimated
225 based on Shannon diversity, observed richness, Faith's phylogenetic diversity and Pielou's evenness using a
226 Kruskal-Wallis test. For beta diversity, a permutational analysis of variance (Adonis) was performed in order to
227 check the significance of the factors ploidy and season, as well as their interaction. In addition, a Permanova test
228 using 999 permutations was performed, and dissimilarities in microbial communities of *S. europaea* (2x) and *S.*
229 *procumbens* (4x) in each sampling season was checked based on Bray-Curtis and Jaccard distances. Principal
230 coordinate analysis (PCoA) plots were visualized in Emperor (Vázquez-Baeza et al. 2013). To define the core
231 microbiome, we considered the definition of Astudillo-García et al. (2017), which defines as part of the core the
232 ASVs present in at least 95% of samples with a minimum 1% relative abundance.

233

234 The files generated in QIIME2 were imported in R (version 3.6.3, R Development Core Team, 2011) using the
235 package Qiime2R (<https://github.com/jbisanz/qiime2R>) and figures were generated using the package ggplot2
236 (Wickham 2016).

237

238 **Results**

239 **Genome size estimation and ploidy**

240 In total, genome size and ploidy of 135 individuals of *Salicornia* was estimated, resulting in 51 diploids (23
241 collected in spring and 28 in summer) and 84 tetraploids (45 collected in spring and 39 in summer). The mean
242 genome size (2C DNA content) \pm standard deviation was 0.652 pg \pm 0.062 for *S. europaea* (2x) and 1.314 pg \pm
243 0.061 for *S. procumbens* (4x).

244

245 **Root anatomical investigation**

246 Significant differences between cytotypes were observed for the following characters: periderma thickness,
247 parenchyma thickness and diameter of vascular cylinder (Table 1). *Salicornia procumbens* (4x) showed thicker
248 periderma and parenchyma layers compared to *S. europaea* (2x), whereas *S. europaea* (2x) had a larger central
249 cylinder compared to *S. procumbens* (4x). The presence of aerenchyma was observed in both *S. europaea* (2x)
250 and *S. procumbens* (4x) (Figure 1).

251

252 **Sequencing results**

253 We initially obtained 1,284,546 sequences. After filtering out the sequences belonging to plants (87.83%) and
254 Cercozoa (0.71%), a total of 145,546 high-quality sequences representing 122 exact amplicon sequence variants
255 (ASVs) were obtained after denoising, merging, and chimera checking. The number of reads per sample ranged
256 from 481 to 13431 with an average of 3093 sequences for *S. procumbens* (4x) and 5703 sequences for *S.*
257 *europaea* (2x) samples. We rarefied the number of reads to 1000 reads per sample. After rarefaction, we
258 remained with eight samples of *S. europaea* (2x) and five samples of *S. procumbens* (4x) collected in spring;
259 and ten samples of *S. europaea* (2x) and seven samples of *S. procumbens* (4x) collected in summer.

260

261 **Alpha and beta diversity of fungal communities**

262 Shannon diversity-based rarefaction curves for both cytotypes showed a plateau at 200 sequences (Figure S1),
263 indicating that sampling depth was enough to cover the diversity of the samples. A similar tendency was
264 observed for richness-based rarefaction curves (Figure S2). Alpha diversity analyses showed higher Shannon
265 Diversity (p=0.012) and Pielou's Evenness (p=0.019) indices in *S. procumbens* (4x) samples compared to *S.*
266 *europaea* (2x) collected in spring (Figure 2). On the other hand, no significant differences but strong trends in

267 the same direction were observed for samples collected in summer (Shannon Diversity Index, $p=0.118$; Pielou's
268 Evenness, $p=0.078$). No significant differences were observed in Faith's Phylogenetic Diversity in spring
269 ($p=0.417$) and summer ($p=0.625$) and observed richness in spring ($p=0.077$) and summer ($p=0.116$) (Figure 2).
270 When the effect of season was analyzed separately for each cytotype, no differences were observed in any of the
271 measured alpha-diversity indices (Table S4).

272

273 Beta diversity analyses showed significant differences in fungal community between the two cytotypes
274 (ADONIS, $p=0.014$), whereas season ($p=0.246$) and the interaction between these factors were not statistically
275 significant ($p=0.604$) (Table 2). In spring, no differences were observed between *S. europaea* (2x) and *S.*
276 *procumbens* (4x) based on Bray-Curtis (Permanova, $p=0.331$, Figure 3A) and Jaccard distances (Permanova,
277 $p=0.476$, Figure 3C); however, in summer, samples of *S. procumbens* (4x) clustered together and significantly
278 differed from that of *S. europaea* (2x) based on both Bray-Curtis (Permanova, $p=0.04$, Figure 3B) and Jaccard
279 distances (Permanova, $p=0.009$, Figure 3D).

280

281 **Core microbiome**

282 We defined the core microbiome as ASVs present in at least 95% of samples with minimum 1% relative
283 abundance in both *S. europaea* (2x) and *S. procumbens* (4x) samples. Overall, 13 ASVs were identified: ten
284 belonging to Ascomycota (unidentified *Xylariales*, *Laburnicola* sp., *Lentithecium pseudoclioninum*,
285 *Cladosporium* sp., *Neocamarosporium* sp., *Alternaria dactyliidicola*, unidentified *Hypocreales*, *Fusarium* sp.,
286 *Plectosphaerella* sp., *Alternaria chlamydospora*) and three to Basidiomycota (unidentified *Malasseziales*,
287 *Wallemia* sp., *Malassezia restricta*). However, there was no core microbiome taxon associated with a single
288 cytotype based on this definition.

289

290 **Taxonomical composition and functional assignment**

291 Fungi belonging to three phyla were detected in the roots of *S. europaea* (2x) (Ascomycota 70.2%,
292 Basidiomycota 29.1% and Chytridiomycota 0.7%) and *S. procumbens* (Ascomycota 60.5%, Basidiomycota
293 36.9% and Chytridiomycota 2.6%). The orders *Xylariales* and *Pleosporales* (Ascomycota), where many DSE
294 fungi are classified, along with *Malasseziales* (Basidiomycota) corresponded to 85% of the sequences in *S.*
295 *europaea* and 75 % in *S. procumbens* (4x) (Figure 4A). Figure 4B shows the taxon bar plots of fungal genera
296 associated with each cytotype in each season. Whereas 25 genera were found to be associated with both

297 cytotypes, six genera were exclusively associated with *S. procumbens* (4x) (Ascomycota: *Lasiodiplodia*,
298 *Didymella*, *Ophiophaerella* and Basidiomycota: *Cystofilobasidium*, *Tausonia*, *Solicoccozyma*) and ten with *S.*
299 *europaea* (2x) (Ascomycota: *Neodidymelliopsis*, *Preussia*, *Trematosphaeria*, *Acremonium* and Basidiomycota:
300 *Kurtzmanomyces*, *Microstroma*, *Rhodotorula*, *Sporobolomyces*, *Itersonilia* and *Papiliotrema*) (Figure 4D).
301 Typical genera of DSE were detected, for example, the genera *Alternaria*, *Cladosporium*, *Ophiophaerella* and
302 *Paraphaeosphaeria*. The majority of the genera were functionally assigned to saprophytic or plant pathogenic
303 trophic modes (Table S5). The most frequent taxon for which it was possible to assign species identity was
304 *Lentithecium pseudoclioninum* (Ascomycota, Pleosporales).

305

306 **Table 1.** Root anatomical characters observed in *S. europaea* (2x) and *S. procumbens* (4x).

Root anatomical characters	<i>S. europaea</i> (2x)	<i>S. procumbens</i> (4x)
maximum root diameter (μm)	2021.78 ± 138.09 a	1908.75 ± 237.12 a
periderma thickness (μm)	108.99 ± 23.73 a	147.28 ± 48.81 b
parenchyma thickness (μm)	180.66 ± 40.79 a	225.83 ± 34.61 b
diameter of vascular cylinder (μm)	1368.82 ± 170.97 a	857.88 ± 246.09 b
diameter of vessels (μm)	24.70 ± 5.05 a	23.93 ± 3.99 a
maximum cell diameter (μm)	33.01 ± 8.07 a	31.24 ± 6.09 a

307 *Data represents mean values ± standard deviation. Values in the same row represented with different letters are
308 statistically different (p < 0.05).

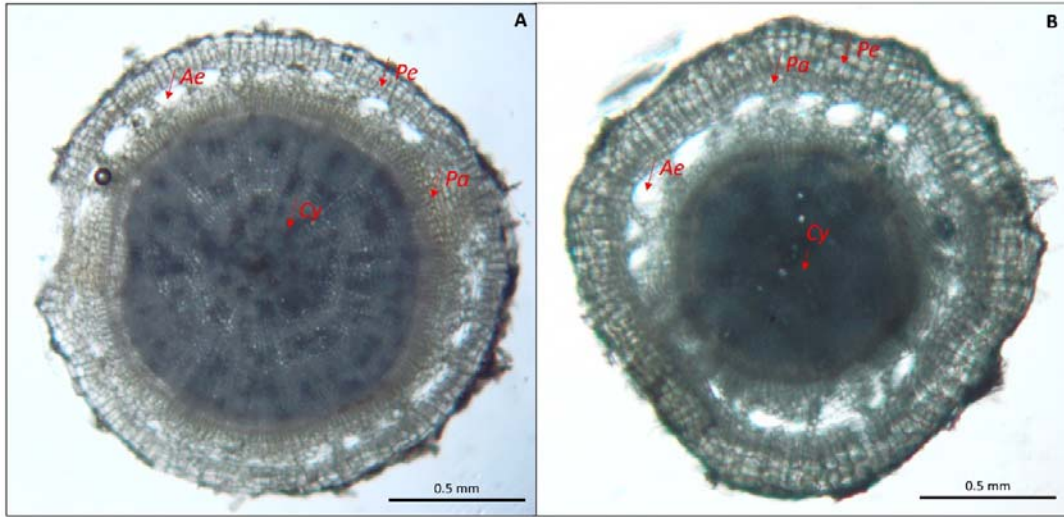
309

310 **Table 2.** Permutational analysis of variance (ADONIS) for the factors season and ploidy.

	D _f	Sum Sq.	Mean Sq.	F model	R ²	P-value
Season	1	0.251	0.251	1.296	0.042	0.246
Ploidy	1	0.529	0.529	2.731	0.088	0.014
Season:Ploidy	1	0.151	0.151	0.779	0.025	0.604
Residuals	33	5.045	0.194		0.843	
Total	36	5.977			1	

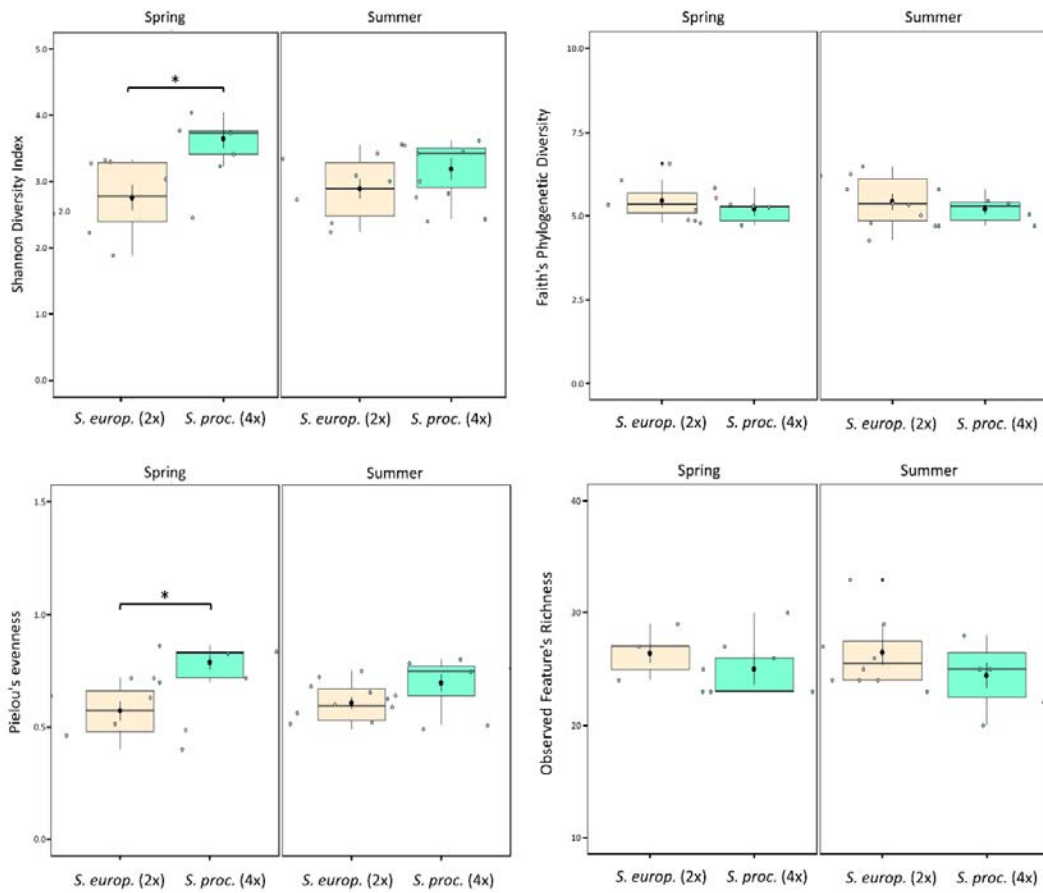
311

312



313

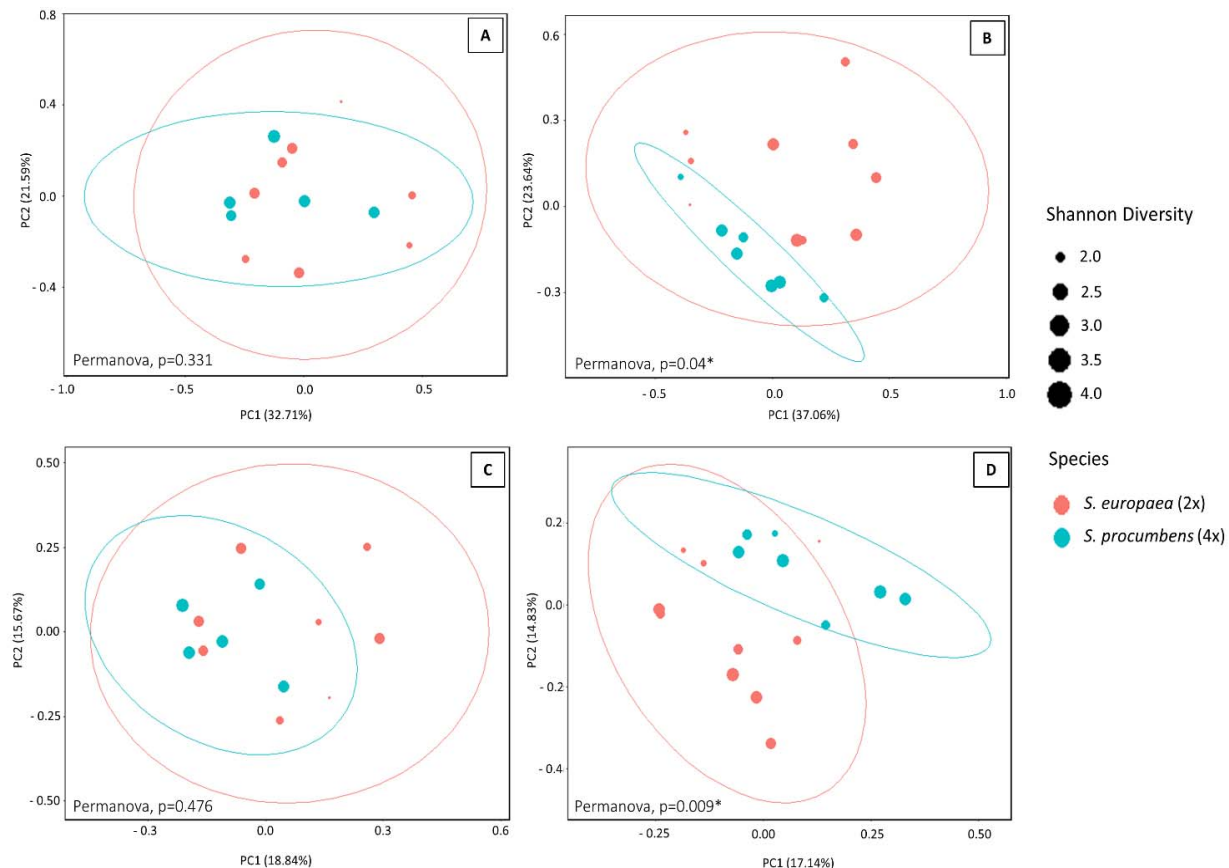
314 **Figure 1.** Root cross-section of *S. europaea* (2x) (A) and *S. procumbens* (4x) (B). *Pe*: periderma; *Pa*:
315 parenchyma; *Ae*: Aerenchyma formation; *Cy*: central cylinder.



316

317 **Figure 2.** Boxplots of Shannon diversity, Faith's phylogenetic diversity, Pielou's evenness and observed
318 richness for *S. europaea* (2x) and *S. procumbens* (4x) in spring and summer. Significant differences (Kruskal-
319 Wallis test, P-value < 0.05) are represented by *.

320



321

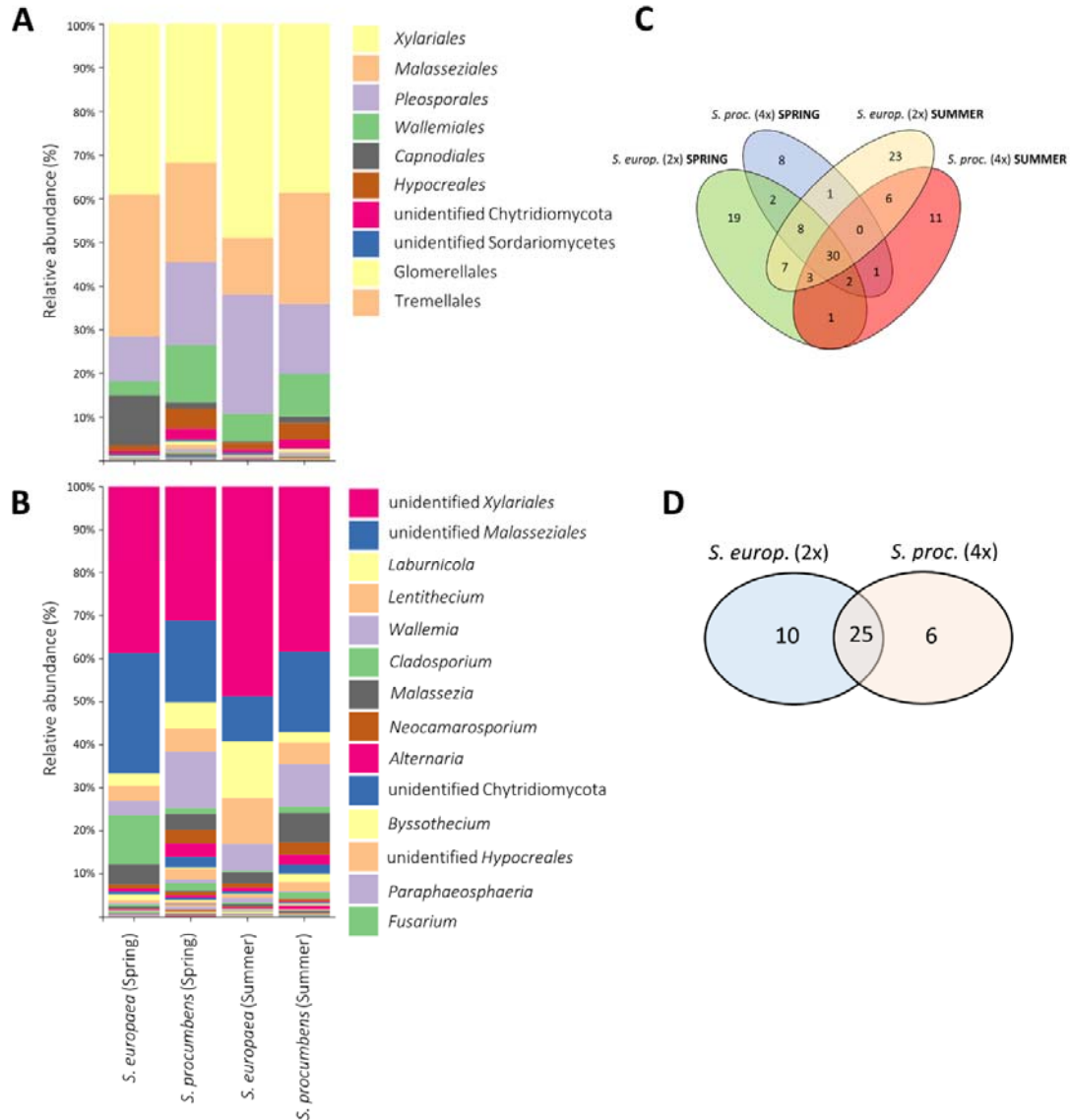
322 **Figure 3.** Principal Coordinate Analysis (PCoA) based on Bray-Curtis distances showing the distribution of
323 fungal communities of *S. europaea* (2x) and *S. procumbens* (4x) in spring (A) and summer (B). PCoA based on
324 Jaccard distances in spring (C) and summer (D). Variation explained by the data in PCoA is presented in
325 percentage.

326

327

328

329



330

331 **Figure 4.** Fungal community composition of *S. europaea* (2x) and *S. procumbens* (4x). **(A)** Relative read
 332 abundance of fungal orders present in each cytotype collected in spring and summer. **(B)** Relative read
 333 abundance of fungal genera present in each cytotype collected in spring and summer. **(C)** Venn diagram of
 334 ASVs associated with each cytotype collected in each season. **(D)** Venn diagram of fungal genera associated
 335 with each cytotype.

336

337

338

339

340

341

342 **Discussion**

343 Polyploidy induces diverse genetic and phenotypic changes in plants. Consequently, there can be cascading
344 effects in their interaction with microorganisms (Segraves & Anneberg 2016), which potentially allows
345 differentiation of polyploids from their diploid relatives. We hypothesized that *S. procumbens* (4x) harbor more
346 diverse fungal communities compared to *S. europaea* (2x) based on greater physiological demands (e.g., higher
347 photosynthetic rates and nutrient requirements) and anatomical differences (e.g., larger cell size) observed in
348 polyploids (Forrester & Ashman 2018; Šmarda et al. 2013). Higher physiological demands may require *S.*
349 *procumbens* (4x) to establish association with a broader range of beneficial fungal partners whereas larger cells
350 provide more space for different fungi to colonize. Our results indicate significant differences in the root-
351 endophytic fungal microbiome associated with *S. procumbens* (4x) and *S. europaea* (2x) in terms of alpha
352 diversity, with *S. procumbens* (4x) samples showing higher Shannon diversity and evenness indices but a trend
353 to lower richness (Fig. 2). This pattern is more prominent in spring suggesting that the fungal community settles
354 by several spring colonizers lost in the year and only few fungi colonizing the plants later. Further, beta
355 diversity analysis showed dissimilar fungal communities associated with *S. procumbens* (4x) and *S. europaea*
356 (2x) samples collected in summer (Fig. 3). However, when the effect of seasonality was independently analyzed,
357 no differences were observed between spring and summer, which indicates comparatively low turnover during
358 the season. The same was reported by Furtado et al. (2019a) when fungal communities colonizing *S. europaea*
359 in spring and autumn were analysed. Finally, we did not observe larger cells in *S. procumbens* (4x) but a thicker
360 parenchyma layer, which suggests a larger area for fungal colonization.

361

362 We investigated cytotype-specific root anatomical traits since previous studies have shown that they can affect
363 microbial recruitment and community assembly. For example, Forrester et al. (2020) noted a greater
364 generalization in bacterial assemblages in autotetraploid individuals of *Medicago sativa* compared to diploids,
365 suggesting that larger cells in polyploids could host a greater quantity of different bacterial symbionts, compared
366 to smaller cells in diploids. In the case of fungi, Galindo-Castañeda et al. (2019) reported a decrease in
367 mycorrhizal colonization in *Zea mays* with a decrease in the living cortical area. In the case of *Salicornia*, our
368 anatomical data showed no differences in cell size between the two cytotypes (Table 1). However, *S. europaea*
369 (2x) showed a larger central cylinder compared to *S. procumbens* (4x) whereas thicker periderma and
370 parenchyma layers were observed in *S. procumbens* (4x) along with an abundant occurrence of aerenchyma (Fig.

371 1, Table 1). We speculate that a thicker periderma and parenchyma, along with the presence of air spaces in *S.*
372 *procumbens* (4x) roots, could provide advantages for endophytes by providing space and oxygen for fungal
373 establishment and survival, especially when the anoxic conditions of salt marshes are considered. Another point
374 to be further investigated is whether the abundant occurrence of aerenchyma, especially in *S. procumbens* (4x),
375 could be due to the presence of specific fungal symbionts. The induction of aerenchyma by fungi was reported
376 by Hu et al. (2018), who observed that the inoculation of rice plants with *Phomopsis liquidambari*
377 (Ascomycota) directly influenced aerenchyma formation via the accumulation of indole-3-acetic acid and
378 ethylene. A similar pattern could also be occurring with *S. procumbens* (4x) but with different fungal symbionts.
379 Although not investigated in this study, host physiology could also be affecting fungal recruitment. Micallef et
380 al. (2019) demonstrated that exudation patterns differed between genotypes of *Arabidopsis thaliana* affecting
381 bacterial recruitment. The same was observed by Zhelnina et al. (2018) in different genotypes of *Avena barbata*.
382 Similar processes are likely to occur with fungi. Since whole-genome duplication can alter root exudation
383 patterns (Jesus-Gonzalez & Weathers 2003), it is possible that in *Salicornia* as well, the two cytotypes produce
384 different root exudates, which consequently leads to different fungal recruitment and community establishment.
385
386 The results of alpha diversity analyses (Fig. 2) showed more diverse and even fungal communities associated
387 with *S. procumbens* (4x) compared to *S. europaea* (2x), although significant differences were observed only in
388 spring. The lower Shannon diversity and evenness observed in *S. europaea* (2x) is seemingly due to the
389 presence of a few and highly dominant fungal taxa colonizing the roots of this cytotype (e.g. unidentified
390 *Xylariales* and *Malasseziales*, *Cladosporium* sp.) but many rare species. This pattern has also been observed in
391 the root-associated bacterial and fungal microbiomes of other plant species (Diaz-Garza et al. 2020, Gobbi et al.
392 2020). Two possible reasons for this are either, highly abundant fungi in *S. europaea* (2x) compact the
393 remaining fungal assemblage, outcompeting other species and reducing community evenness. Alternatively, the
394 roots of the diploid species form a specialized environment allowing only a few species to establish. Beta
395 diversity analyses showed that fungal communities clustered according to cytotype and did not cluster according
396 to season (Table 2). Other studies investigating the influence of seasonality in shaping root-endophytic fungal
397 microbiomes in *Salicornia* also showed that community composition and structure remained stable over the
398 complete *Salicornia patula* lifecycle (Maciá-Vicente et al. 2016) and in the case of *S. europaea*, it did not change
399 between spring and autumn (Furtado et al. 2019a). Thus, despite being annual these plants seem not to be

400 limited by a lack of mutualistic endophytic fungi in the early season but are also immediately affected by
401 pathogenic fungi.

402

403 The core microbiome of *Salicornia* comprised 13 ASVs. Some of these taxa have been already reported
404 colonizing *Salicornia* spp. such as *Alternaria chlamydospora* (Furtado et al. 2019a), *Cladosporium* sp. (Furtado
405 et al. 2019b; Maciá-Vicente et al. 2016) and *Fusarium* sp. (Furtado et al. 2019b). In addition, other taxa detected
406 in our study have been reported colonizing other chenopod hosts, such as *Laburnicola* sp. isolated from *Suaeda*
407 *salsa* (Yuan et al. 2020) and *Neocamarosporium* sp. isolated from *Atriplex portulacoides* (Gonçalves et al.
408 2019). We detected some ASVs exclusively associated with each cytotype. For example, an unidentified ASV
409 belonging to Tremellomycetes was detected in five samples of *S. europaea* (2x). The same was observed for a
410 unidentified ASV belonging to Pleosporales in *S. procumbens* (4x). Nevertheless, these do not constitute
411 cytotype-specific core microbiomes since these ASVs were not detected in more than 95% of the samples of
412 each cytotype. Apart from the genera *Alternaria* sp. and *Fusarium* sp., well known as plant pathogens but also
413 reported as mutualists (Mendoza & Siroka 2009; Musetti et al. 2007) and the genus *Laburnicola* sp., reported in
414 a mutualistic association with the halophyte *Suaeda salsa* (Yuan et al. 2020), the other taxa present in the
415 *Salicornia* core microbiome are mostly considered saprotrophs (e.g., order *Xylariales*, *Cladosporium* sp.,
416 *Lentithecium* sp.) or plant pathogens (e.g., *Cladosporium* sp.).

417

418 As observed for the core microbiome, functional assignment revealed that most of the genera detected in our
419 samples were classified in two trophic modes: saprotroph or pathotroph. However, two genera (*Alternaria* and
420 *Fusarium*) colonizing both *S. europaea* (2x) and *S. procumbens* (4x), and *Acremonium*, detected in roots of only
421 *S. europaea* (2x), were classified into the pathotroph-saprotroph-symbiotroph trophic mode, according to
422 FunGuild database (Nguyen et al. 2016). The outcome of the plant-fungal association is known to depend on a
423 set of abiotic and biotic factors (Hardoim et al. 2015). Studies have shown that fungi may change lifestyle (e.g.,
424 from mutualistic to pathogenic) depending on host, plant genotype, environmental conditions and the dynamic
425 network of interactions within the plant microbiome (Fesel & Zuccaro 2016; Hardoim et al. 2015), whereas the
426 effect of whole-genome duplication in this regard is still unknown. Physiological characteristics inherent to each
427 host, for example, the differences in fungal gene expression in response to the host or differences in plant's
428 ability to respond to the fungus, has been shown to play a major role in controlling the outcome of the symbiosis
429 (Redman et al. 2001). Interestingly, plant physiology is known to differ between diploids and polyploids (Baker

430 et al. 2017), although not yet explored in *Salicornia*. It is possible that cytotype-specific physiological
431 characteristics in *Salicornia*, such as different nutrient requirements, could modulate in different ways the
432 symbiotic interaction with endophytic fungi.

433

434 We hypothesized that in the salt marsh context, *S. procumbens* (4x) has a larger microscale distribution, possibly
435 due to its association with more or more generalized mutualistic fungi. However, there are no studies to
436 investigate whether establishing symbiosis with beneficial fungi is also part of the strategy adopted by
437 polyploids to colonize different habitats. In the case of *Salicornia*, Teege et al. (2011) detected an ecologically
438 differentiated distribution of two closely-related *Salicornia* species in the salt marsh zones suggesting a strong
439 selection during seed germination and seedling establishment as reasons for the habitat differentiation.
440 Nevertheless, there is no information regarding the influence of belowground interactions in this regard. Since
441 polyploids have higher demands for nutrients in order to synthesize additional chromosomal sets (Guignard et
442 al. 2016; Šmarda et al. 2013), associating with mutualistic fungi could be part of their strategy to fulfil the
443 nutrient requirements and increase its competitiveness. Our results showed that *S. procumbens* (4x) did not
444 associate specifically with mutualistic fungal symbionts. This finding leaves the possibility that either the
445 assignments to guilds are inexact

446 because of the high functional differences at species or genus level or fungal endophytes are not contributing or
447 are playing a minor role in *S. procumbens* (4x) colonization of harsh habitats, such as tidal flats where frequent
448 flooding associated to high salinity occur. However, we cannot exclude that association with mutualistic fungi is
449 habitat-dependent. Therefore, in a next step, sampling of *Salicornia* across the salt marsh into the pioneer zone
450 and tidal flats would be necessary to understand whether mutualists are more abundant in roots of tetraploid
451 plants colonizing harsher parts of the salt marsh and not the LSM.

452

453 Overall, our results corroborate past work in which polyploid plants were found to harbor more diverse root-
454 associated endophytic communities compared to diploids, not only fungi (Těšitelová et al. 2013) but also
455 bacteria (Wipf & Coleman-Derr 2021). However, further research should consider including samples of *S.*
456 *europaea* (2x) and *S. procumbens* (4x) collected in different populations. This would allow for drawing
457 conclusions in a broader ecological context. In addition to that, further investigations are necessary to elucidate
458 the exact anatomical or physiological mechanisms inherent to each cytotype and responsible for these
459 differences. It is possible that larger parenchyma observed in *S. procumbens* (4x) could provide more space for

460 fungal colonization also benefiting nutrient uptake. To support this hypothesis, further work under controlled
461 conditions is necessary to investigate whether *S. procumbens* (4x) has different physiological demands (e.g.,
462 higher nutrient requirements) compared to *S. europaea* (2x). Finally, since DNA-based methods do not provide
463 information on the active root-inhabiting fungi colonizing each cytotype, transcriptomic analyses would help us
464 to understand whether fungal communities are dominated in their activity by few species and whether different
465 active fungal community profiles occur in the two cytotypes.

466

467 **References**

468 Abarenkov K, Zirk A, Piirmann T, Pöhönen R, Ivanov F, Nilsson RH, Kõljalg U (2020) UNITE QIIME release
469 for Fungi. Version 04.02.2020. UNITE Community. <https://doi.org/10.15156/BIO/786385>

470

471 Anneberg TJ, Segraves KA (2019) Intraspecific polyploidy correlates with colonization by arbuscular
472 mycorrhizal fungi in *Heuchera cylindrica*. Am J Bot 106:894-900. <https://doi.org/10.1002/ajb2.1294>

473

474 Astudillo-García C, Bell JJ, Webster NS, Glasl B, Jompa J, Montoya JM, Taylor MW (2017) Evaluating the
475 core microbiota in complex communities: a systematic investigation. Environ Microbiol 19:1450-1462.
476 <https://doi.org/10.1111/1462-2920.13647>

477

478 Baker RL, Yarkhunova Y, Vidal K, Ewers BE, Weinig C (2017) Polyploidy and the relationship between leaf
479 structure and function: implications for correlated evolution of anatomy, morphology, and physiology in
480 *Brassica*. BMC Plant Biol 17:3. <https://doi.org/10.1186/s12870-016-0957-3>

481

482 Baranyi M, Greilhuber J (1996) Flow cytometric and Feulgen densitometric analysis of genome size variation in
483 *Pisum*. Theor App Genet 92:297–307. <https://doi.org/10.1007/BF00223672>.

484

485 Bolyen E, Rideout JR, Dillon MR, Bokulich NA, Abnet CC, Al-Ghalith GA, Alexander H, Alm EJ, Arumugam
486 M, Asnicar F, Bai Y, Bisanz JE, Bittinger K, Brejnrod A, Brislawn CJ, Brown CT, Callahan BJ, Caraballo-
487 Rodríguez AM, Chase J, Cope EK, Da Silva R, Diener C, Dorrestein PC et al (2019) Reproducible, interactive,
488 scalable and extensible microbiome data science using QIIME 2. Nat Biotechnol 37:852–857.
489 <https://doi.org/10.1038/s41587-019-0209-9>

490

491 Buhk N (2020) Effects of genetic diversity on colonization, distribution and coexistence of two cytotypes of
492 glasswort (*Salicornia* L.). Dissertation, Carl von Ossietzky University of Oldenburg.

493

494 Bushnell B, Rood J, Singer E (2017) BBMerge - accurate paired shotgun read merging via overlap. Plos One,
495 12: e0185056. <https://doi.org/10.1371/journal.pone.0185056>

496

497 Callahan B, McMurdie P, Holmes S (2017) Exact sequence variants should replace operational taxonomic units
498 in marker-gene data analysis. ISME J 11:2639–2643. <https://doi.org/10.1038/ismej.2017.119>

499

500 Cavé-Radet A, Correa-Garcia S, Monard C, El Amrani A, Salmon A, Ainouche M, Yergeau E (2020)
501 Phenanthrene contamination and ploidy level affect the rhizosphere bacterial communities of *Spartina* spp.
502 FEMS Microbiol Ecol: fiaa156. <https://doi.org/10.1093/femsec/fiaa156>

503

504 Chansler MT, Ferguson CJ, Fehlberg SD, Prather LA (2016) The role of polyploidy in shaping morphological
505 diversity in natural populations of *Phlox amabilis*. Am J Bot 103: 1546-1558.
506 <https://doi.org/10.3732/ajb.1600183>

507

508 Collins AR, Müller-Schärer H (2012) Influence of plant phenostage and ploidy level on oviposition and feeding
509 of two specialist herbivores of spot-ted knapweed *Centaurea stoebe*. Biol Control 60:148-153.
510 <https://doi.org/10.1016/j.biocontrol.2021.104728>

511

512 Corneillie S, De Storme N, Van Acker R, Fangel JU, De Bruyne M, De Rycke R, Geelen D, Willats WGT,
513 Vanholme B, Boerjan W (2019) Polyploidy affects plant growth and alters cell wall composition. Plant Physiol
514 179:74-87. <https://doi.org/10.1104/pp.18.00967>

515

516 Crous PW, Verkleij GJM, Groenewald JZ (2009) Fungal biodiversity, CBS laboratory Manual Series 1, CBS-
517 KNAW Fungal Biodiversity Centre, Utrecht, The Netherlands.

518

519 Diaz-Garza AM, Fierro-Rivera JI, Pacheco A, Schüßler A, Gradilla-Hernández MS, Senés-Guerrero C (2020)
520 Temporal dynamics of *Rhizobacteria* found in pequin pepper, soybean and orange trees growing in a semi-arid
521 ecosystem. Front Sustain Food Sys 4:602283. <https://doi.org/10.3389/fsufs.2020.602283>

522

523 Doyle JJ, Coate JE (2019) Polyploidy, the nucleotype, and novelty: The impact of genome doubling on the
524 biology of the cell. Int J Plant Sci 180:1-52. <https://doi.org/10.1086/700636>

525

526 Edger PP, Heidel-Fischer HM, Bekaert M, Rota J, Glöckner G, Platts AE, Heckel DG, Der JP, Wafula EK, Tang
527 M, Hofberger JA, Smithson A, Hall JC, Blanchette M et al. (2015) The butterfly plant arms-race escalated by
528 gene and genome duplications. PNAS 112:8362–8366. <https://doi.org/10.1073/pnas.1503926112>

529

530 Fesel PH, Zuccaro A (2016) Dissecting endophytic lifestyle along the parasitism/mutualism continuum in
531 *Arabidopsis*. Curr Opin Microbiol 32:103-112. <https://doi.org/10.1016/j.mib.2016.05.008>

532

533 Forrester NJ, Ashman TL (2018) The direct effects of plant-polyploidy on the legume-rhizobia mutualism. Ann
534 Bot 121:209-220. <https://doi.org/10.1093/aob/mcx121>

535

536 Forrester NJ, Ashman TL (2019) Autopolyploidy alters nodule-level interaction in the legume-rhizobium
537 mutualism. *Am J Bot* 107:179-185. <https://doi.org/10.1002/ajb2.1375>

538

539 Forrester NJ, Rebolleda-Gómez M, Sachs JL, Ashman T-L (2020) Polyploid plants obtain greater fitness
540 benefits from a nutrient acquisition mutualism. *New Phytol* 227: 944-954. <https://doi.org/10.1111/nph.16574>

541

542 Furtado BU, Golebierski M, Skorupa M, Hulisz P, Hrynkiewicz K (2019a) Bacterial and Fungal endophytic
543 microbiomes of *Salicornia europaea*. *AEM* 85:e00305-19. <https://doi.org/10.1128/AEM.00305-19>

544

545 Furtado BS, Szymańska S, Hrynkiewicz K (2019b) A window into fungal endophytism in *Salicornia europaea*:
546 deciphering fungal characteristics as plant growth promoting agents. *Plant Soil* 445:577-594.
547 <https://doi.org/10.1007/s11104-019-04315-3>

548

549 Galindo-Castañeda T, Brown KM, Kuldau GA, Roth GW, Wenner NG, Ray S, Schneider H, Lynch JP (2019)
550 Root cortical anatomy is associated with differential pathogenic and symbiotic fungal colonization in maize.
551 *Plant Cell Environ* 42:2999-3014. <https://doi.org/10.1111/pce.13615>

552

553 Gobbi A, Kyrkou I, Filippi E, Ellegaard-Jensen L, Hansen LH (2020) Seasonal epiphytic microbial dynamics on
554 grapevine leaves under biocontrol and copper fungicide treatments. *Sci Rep* 10:681.
555 <https://doi.org/10.1038/s41598-019-56741-z>

556

557 Gonçalves DR, Pena R, Zott G, Albach D (2021) Effects of fungal inoculation on the growth of *Salicornia*
558 (Amaranthaceae) under different salinity conditions. *Symbiosis* 84:195-208. <https://doi.org/10.1007/s13199-021-00783-3>

560

561 Gonçalves FF, Aleixo A, Vicente TFL, Esteves AC, Alves A (2019) Three new species of *Neocamarosporium*
562 isolated from saline environments: *N. aestuarium* sp. nov., *N. endophyticum* sp. nov. and *N. halimiones* sp. nov.
563 *Mycosphere* 10:608-621. <https://doi.org/10.5943/mycosphere/10/1/11>

564

565 Guignard MS, Nichols RA, Knell RJ, Macdonald A, Romila CA, Trimmer M, Leitch IJ, Leitch AR (2016)
566 Genome size and ploidy influence angiosperm species' biomass under nitrogen and phosphorus limitation. *New
567 Phytol* 210:1195-1206. <https://doi.org/10.1111/nph.13881>

568

569 Hardoim PR, van Overbeek L, Berg G, Pirttilä AM, Compañt S, Campisano A, Döring M, Sessitsch A (2015)
570 The hidden world within plants: ecological and evolutionary considerations for defining functioning of
571 microbial endophytes. *Microbiol Mol Biol R* 79:293-320. <https://doi.org/10.1128/MMBR.00050-14>

572

573 Hu L-Y, Li D, Sun K, Cao W, Fu WQ, Zhang W, Dai C-C (2018) Mutualistic fungus *Phomopsis liquidambari*
574 increases root aerenchyma formation through auxin-mediated ethylene accumulation in rice (*Oryza sativa* L.).
575 *Plant Physiol Biochem* 130:367-376. <https://doi.org/10.1016/j.plaphy.2018.07.018>

576

577 Husband BC, Schemske DW (2000) Ecological mechanisms of reproductive isolation between diploid and

578 tetraploid *Chamerion angustifolium*. *J Ecol* 88:689-701. <https://doi.org/10.1046/j.1365-2745.2000.00481.x>

579

580 Jesus-Gonzalez L, Weathers PJ (2003) Tetraploid *Artemisia annua* hairy roots produce more artemisinin than

581 diploids. *Plant Cell Rep* 21:809-813. <https://doi.org/10.1007/s00299-003-0587-8>

582

583 Kadereit G, Ball P, Beer S, Mucina L, Sokoloff D, Teege P, Yaprak AE, Freitag H (2007) A taxonomic

584 nightmare comes true: phylogeny and biogeography of glassworts (*Salicornia* L., Chenopodiaceae). *Taxon*

585 56:1143–1170. <https://doi.org/10.2307/25065909>

586

587 Kao RH (2008) Implications of polyploidy in the host plant of a dipteran seed parasite. *West N Am Nat* 68:225-

588 230.

589

590 Kennedy BF, Sabara HA, Haydon D, Husband BC (2006) Pollinator-mediated assortative mating in mixed

591 ploidy populations of *Chamerion angustifolium* (Onagraceae). *Oecologia* 150:398-408.

592 <https://doi.org/10.1007/s00442-006-0536-7>

593

594 Maciá-Vicente JG, Nam B, Thines M (2020) Community sequencing on a natural experiment reveals little

595 influence of host species and timing but a strong influence of compartment on the composition of root

596 endophytes in three annual *Brassicaceae*. *BioRxiv*. doi: <https://doi.org/10.1101/2020.01.24.918177>

597

598 Maciá-Vicente JG, Nau T, Piepenbring M (2016) Low diversity and abundance of root endophytes prevail

599 throughout the lifecycle of an annual halophyte. *Mycol Prog* 15:1303-1311. <https://doi.org/10.1007/s11557-016-1241-5>

600

601

602 Mateu MG, Baldwin AH, Maul JE, Yarwood SA (2020) Dark septate endophytes improve salt tolerance of

603 native and invasive lineages of *Phragmites australis*. *ISME J* 14:1943-1954. <https://doi.org/10.1038/s41396-020-0654-y>

604

605

606 Mendoza AR, Sikora RA (2009) Biological control of *Radopholus similis* in banana by combined application of

607 the mutualistic endophyte *Fusarium oxysporum* strain 162, the egg pathogen *Paecilomyces lilacinus* strain 251

608 and the antagonistic bacteria *Bacillus firmus*. *BioControl* 54:263-272. <https://doi.org/10.1007/s10526-008-9181-x>

609

610

611 Meudt HM, Rojas-Andrés BM, Prebble JM, Low E, Garnock-Jones PJ, Albach DC (2015) Is genome

612 downsizing associated with diversification in polyploid lineages of *Veronica*? *Bot J Linn Soc* 178:243-266.

613 <https://doi.org/10.1111/boj.12276>

614

615 Micallef SA, Shiaris MP, Colón-Carmona A (2019) Influence of *Arabidopsis thaliana* accessions on
616 rhizobacterial communities and natural variation in root exudates. *J Exp Bot* 60:1729-1742.
617 <https://doi.org/10.1093/jxb/erp053>

618

619 Musetti R, Polizzotto R, Vecchione A, Borselli S, Zulini L, D'Ambrosio M, Toppi L, Pertot I (2007) Antifungal
620 activity of diketopiperazines extracted from *Alternaria alternata* against *Plasmopora viticola*: an ultrastructural
621 study. *Micron* 38:643-650. <https://doi.org/10.1016/j.micron.2006.09.001>

622

623 Nord EA, Lynch JP (2009) Plant phenology: a critical controller of soil resource acquisition. *J Exp Bot* 60:
624 1927-1937. <https://doi.org/10.1093/jxb/erp018>

625

626 Nguyen NH, Song Z, Bates ST, Branco S, Tedersoo L, Menke J, Schilling JS, Kennedy PG (2016) FUNGuild:
627 an open annotation tool for parsing fungal community datasets by ecological guild. *Fungal Ecol* 20:241-248.
628 <https://doi.org/10.1016/j.funeco.2015.06.006>

629

630 Pöhlme S, Abarenkov K, Nilsson RH, Lidahl BD, Klemmensen KE, Kauserud H, Nguyen N, Kjoller R, Bates
631 ST, Baldrian P et al. (2021) FungalTraits: a user friendly database of fungi and fungus-like stramenopiles.
632 *Fungal Divers* 105:1-16. <https://doi.org/10.1007/s13225-020-00466-2>

633

634 R Development Core Team (2011) A language and environment for statistical computing. Vienna, Austria: R
635 Foundation for statistical computing. Available from: <https://www.R-project.org>.

636

637 Redman RS, Dunigan DD, Rodriguez RJ (2001) Fungal symbiosis from mutualism to parasitism: who controls
638 the outcome, host or invader? *New Phytol* 151:705-716. <https://doi.org/10.1046/j.0028-646x.2001.00210.x>

639

640 Reynolds HL, Packer A, Bever JD, Clay K (2003) Grassroots ecology: Plant-microbe-soil interactions as drivers
641 of plant community structure and dynamics. *Ecology* 84:2281-2291. <https://doi.org/10.1890/02-0298>

642

643 Rivers AR, Weber KC, Gardner TG, Liu S, Armstrong SD (2018) ITSxpress: Software to rapidly trim
644 internally transcribed spacer sequences with quality scores for marker gene analysis. *F1000Research*
645 7:1418. <https://doi.org/10.12688/f1000research.15704.1>

646

647 Segraves KA, Anneberg TJ (2016) Species interactions and plant polyploidy. *Am J Bot* 103:1326-1335.
648 <https://doi.org/10.3732/ajb.1500529>

649

650 Šmrda P, Hejcmán M, Březinová A, Horová L, Steigerová H, Zedek F, Bureš P, Hejcmánová P, Schellberg J
651 (2013) Effect of phosphorus availability on the selection of species with different ploidy levels and genome
652 sizes in a long-term grassland fertilization experiment. *New Phytol* 200:911-921.
653 <https://doi.org/10.1111/nph.12399>

654

655 Sudová R, Rydlova J, Münzbergová Z, Suda J (2010) Ploidy-specific interactions of three host plants with
656 arbuscular mycorrhizal fungi: Does genome copy number matter? Am J Bot 97:1798–1807.
657 <https://doi.org/10.3732/ajb.1000114>

658

659 Sudová R, Pankova H, Rydlova J, Münzbergová Z, Suda J (2014) Intraspecific ploidy variation: a hidden, minor
660 player in plant–soil–mycorrhizal fungi interactions. Am J Bot 101:26–33. <https://doi.org/10.3732/ajb.1300262>

661

662 Sudová R, Kohout P, Kolaříková Z, Rydlová J, Vorříšková J, Suda J, Španiel S, Müller-Schärer H, Mráz P
663 (2018) Sympatric diploid and tetraploid cytotypes of *Centaurea stoebe* s.l. do not differ in arbuscular
664 mycorrhizal communities and mycorrhizal growth response. Am J Bot 105:1995–2007.
665 <https://doi.org/10.1002/ajb2.1206>

666

667 Teege P, Kadereit JW, Kadereit G (2011) Tetraploid European *Salicornia* species are best interpreted as
668 ecotypes of multiple origin. Flora 206:910–920. <https://doi.org/10.1016/j.flora.2011.05.009>

669

670 Těšitelová T, Jersáková J, Roy M, Kubátová B, Těšitel J, Urfus T, Trávníček P, Suda J (2013) Ploidy-specific
671 symbiotic interactions: divergence of mycorrhizal fungi between cytotypes of the *Gymnadenia conopsea* group
672 (Orchidaceae). New Phytol 199:1022–1033. <https://doi.org/10.1111/nph.12348>

673

674 Toju H, Tanabe AS, Yamamoto S, Sato H (2012) High coverage ITS primers for the DNA-based identification
675 of Ascomycetes and Basidiomycetes in environmental samples. Plos One 7: e40863.
676 <https://doi.org/10.1371/journal.pone.0040863>

677

678 van Loon LC, Rep M, Pieterse CMJ (2006) Significance of inducible defense-related proteins in infected plants.
679 Annu Rev Phytopathol 44:135–162. <https://doi.org/10.1146/annurev.phyto.44.070505.143425>

680

681 Vancov T, Keen B (2009) Amplification of soil fungal community DNA using the ITS86F and ITS4 primers.
682 FEMS Microbiol Lett 296:91–96. <https://doi.org/10.1111/j.1574-6968.2009.01621.x>

683

684 Vázquez-Baeza Y., Pirrung M., Gonzalez A., Knight R. 2013. Emperor: A tool for visualizing high-throughput
685 microbial community data. Gigascience 2:16. <https://doi.org/10.1186/2047-217X-2-16>

686

687 Veach AM, Yip D, Engle NL, Yang ZK, Bible A, Morrel-Favye J, Tschaplinski TJ, Kalluri UC, Schadt CW
688 (2018) Modification of plant cell wall chemistry impacts metabolome and microbiome composition in *Populus*
689 *PdKOR1* RNAi plants. Plant Soil, 429:349–361. <https://doi.org/10.1007/s11104-018-3692-8>

690

691 Vergara C, Araujo KEC, Sperandio MVL, Santos LA, Urquiaga S, Zilli JE (2019) Dark septate endophytic
692 fungi increase the activity of proton pumps, efficiency of ¹⁵N recovery from ammonium sulphate, N content, and
693 micronutrient levels in rice plants. Braz J Microbiol 50:825–838. <https://doi.org/10.1007/s42770-019-00092-4>

694

695 Wickham H (2016) *ggplot2: elegant graphics for data analysis*. New York: Springer-Verlag.
696 <https://ggplot2.tidyverse.org/>

697

698 Wildermuth MC (2010) Modulation of host nuclear ploidy: A common plant biotroph mechanism. *Curr Opin*
699 *Plant Biol* 13:449-458. <https://doi.org/10.1016/j.pbi.2010.05.005>

700

701 Wipf HML, Coleman-Derr D (2021) Evaluating domestication and ploidy effects on the assembly of the wheat
702 bacterial microbiome. *Plos One* 16:e0248030. <https://doi.org/10.1371/journal.pone.0248030>

703

704 Yuan Z, Druzhinina IS, Wang X, Zhang X, Peng L, Labb   J (2020) Insight into a highly polymorphic endophyte
705 isolated from the roots of the halophytic seepweed *Suaeda salsa*: *Laburnicola rhizohalophila* sp. nov.
706 (Didymosphaeriaceae, Pleosporales). *Fungal Biol* 124:327-337. <https://doi.org/10.1016/j.funbio.2019.10.001>

707

708 Zhalnina K, Louie KB, Hao Z, Mansoori N, Rocha UN, Shi S, Cho H, Karaoz U, Loqu   D, Bowen BP,
709 Firestone MK, Northen TR, Brodie EL (2018) Dynamic root exudate chemistry and microbial substrate
710 preferences drive patterns in rhizosphere microbial community assembly. *Nat Microbiol* 3:470-480.
711 <https://doi.org/10.1038/s41564-018-0129-3>

712

713 **Declarations**

714 **Funding**

715 Funding was provided by the German Research Foundation (Research Unit DynaCom FOR 2716: Spatial
716 community ecology in highly dynamic landscapes: from island biogeography to metaecosystems).

717 **Availability of data and material**

718 All raw sequences are available from BioProject ID: PRJNA764035.

719 **Author contributions**

720 DRG and DCA planned and designed the study with suggestions provided by RP. DRG performed sampling,
721 molecular work, data analyses and wrote the first draft. DRG, RP and DCA contributed to the final version of
722 the manuscript.

723 **Acknowledgements**

724 We would like to thank Sabrina Sch  ngart for performing the ploidy measurements and Eike Mayland-
725 Quellhorst for his help with molecular work. We also thank the administration of the Lower Saxony Wadden Sea
726 National Park for allowing us to collect the samples used in this study.

727